STRUCTURAL SCIENCE
CRYSTAL ENGINEERING
MATERIALS

Volume 74 (2018)

Supporting information for article:

Revisiting the I{\overline 1} structures of high-temperature Ca-rich plagioclase feldspar – a single-crystal neutron and X-ray diffraction study

Shiyun Jin, Xiaoping Wang and Huifang Xu

Table S1 Electron microprobe analyses results

	Weight%							Formula normalized to 8 oxygen							Composition
	SiO_2	Al_2O_3	FeO	CaO	Na_2O	K_2O	Totals	Si	Al	Fe	Ca	Na	K	Totals	
Lake Co. *e*2	51.068	30.751	0.403	12.941	3.957	0.144	99.264	2.337	1.659	0.015	0.635	0.351	0.008	12.997	$An_{63.8}Ab_{35.3}Or_{0.8}$
	51.147	30.478	0.553	13.071	3.899	0.107	99.254	2.342	1.645	0.021	0.641	0.346	0.006	12.993	$An_{64.5}Ab_{34.8}Or_{0.6}$
	51.582	30.422	0.513	12.986	3.875	0.110	99.489	2.354	1.636	0.020	0.635	0.343	0.006	12.985	$An_{64.5}Ab_{34.8}Or_{0.6}$
	51.821	30.454	0.520	13.215	3.974	0.110	100.094	2.353	1.630	0.020	0.643	0.350	0.006	12.991	$An_{64.3}Ab_{35.0}Or_{0.6}$
	50.924	30.432	0.413	13.040	3.944	0.139	98.893	2.340	1.648	0.016	0.642	0.351	0.008	12.995	$An_{64.1}Ab_{35.1}Or_{0.8}$
	51.293	30.279	0.456	13.202	4.048	0.138	99.416	2.347	1.633	0.017	0.647	0.359	0.008	13.002	$An_{63.8}Ab_{35.4}Or_{0.8}$
Lake Co. $I\bar{1}$	50.523	30.856	0.462	13.366	3.579	0.114	98.900	2.325	1.674	0.018	0.659	0.319	0.007	13.001	$An_{66.9}Ab_{32.4}Or_{0.7}$
	50.175	30.699	0.375	13.669	3.558	0.119	98.594	2.319	1.672	0.015	0.677	0.319	0.007	13.008	$An_{67.5}Ab_{31.8}Or_{0.7}$
	50.878	30.844	0.503	13.814	3.701	0.117	99.857	2.324	1.660	0.019	0.676	0.328	0.007	13.014	$An_{66.9}Ab_{32.4}Or_{0.7}$
	50.653	31.197	0.457	13.591	3.670	0.095	99.663	2.315	1.681	0.017	0.666	0.325	0.006	13.010	$An_{66.8}Ab_{32.6}Or_{0.6}$
	50.854	30.617	0.594	13.590	3.596	0.100	99.351	2.332	1.655	0.023	0.668	0.320	0.006	13.003	$An_{67.2}Ab_{32.2}Or_{0.6}$
	51.080	30.631	0.472	13.651	3.598	0.116	99.547	2.337	1.651	0.018	0.669	0.319	0.007	13.001	$An_{67.3}Ab_{32.1}Or_{0.7}$
28-88	51.698	30.920	0.458	13.607	3.804	0.163	100.649	2.339	1.649	0.017	0.660	0.334	0.009	13.008	$An_{65.8}Ab_{33.3}Or_{0.9}$
	51.293	30.777	0.411	13.642	3.690	0.132	99.944	2.337	1.652	0.016	0.666	0.326	0.008	13.004	$An_{66.6}Ab_{32.6}Or_{0.8}$
	50.391	30.783	0.444	13.649	3.657	0.152	99.076	2.319	1.670	0.017	0.673	0.326	0.009	13.014	$An_{66.7}Ab_{32.4}Or_{0.9}$
	50.872	30.668	0.412	13.748	3.709	0.178	99.586	2.329	1.655	0.016	0.674	0.329	0.010	13.013	$An_{66.5}Ab_{32.5}Or_{1.0}$
	51.264	30.889	0.397	13.719	3.752	0.127	100.148	2.332	1.656	0.015	0.669	0.331	0.007	13.009	$An_{66.4}Ab_{32.9}Or_{0.7}$
	50.874	30.427	0.513	13.690	3.752	0.145	99.400	2.334	1.645	0.020	0.673	0.334	0.008	13.014	$An_{66.3}Ab_{32.9}Or_{0.8}$
55-88	48.651	32.203	0.303	15.327	2.741	0.038	99.263	2.242	1.749	0.012	0.757	0.245	0.002	13.007	$An_{75.4}Ab_{24.4}Or_{0.2}$
	49.186	32.584	0.262	15.300	2.915	0.057	100.304	2.243	1.751	0.010	0.747	0.258	0.003	13.012	$An_{74.1}Ab_{25.6}Or_{0.3}$
	49.170	32.241	0.349	15.166	2.693	0.032	99.650	2.254	1.742	0.013	0.745	0.239	0.002	12.996	$An_{75.5}Ab_{24.3}Or_{0.2}$
	49.171	32.489	0.343	15.425	2.772	0.060	100.261	2.244	1.747	0.013	0.754	0.245	0.004	13.007	$An_{75.2}Ab_{24.5}Or_{0.3}$
	49.425	32.070	0.303	15.173	2.613	0.053	99.637	2.264	1.732	0.012	0.745	0.232	0.003	12.987	$An_{76.0}Ab_{23.7}Or_{0.3}$
7155	48.950	32.181	0.400	15.133	2.679	0.048	99.390	2.248	1.742	0.015	0.745	0.239	0.003	12.983	$An_{75.5}Ab_{24.2}Or_{0.3}$
	49.412	32.521	0.363	15.030	2.752	0.053	100.130	2.251	1.746	0.014	0.734	0.243	0.003	12.983	$An_{74.9}Ab_{24.8}Or_{0.3}$
	48.922	32.253	0.355	15.114	2.718	0.090	99.451	2.247	1.746	0.014	0.744	0.242	0.005	12.994	$An_{75.0}Ab_{24.4}Or_{0.5}$
	48.792	32.213	0.300	14.970	2.828	0.056	99.157	2.246	1.748	0.012	0.738	0.252	0.003	12.992	$An_{74.3}Ab_{25.4}Or_{0.3}$
	49.253	32.075	0.393	14.968	2.744	0.060	99.493	2.258	1.733	0.015	0.735	0.244	0.004	12.979	$An_{74.8}Ab_{24.8}Or_{0.4}$

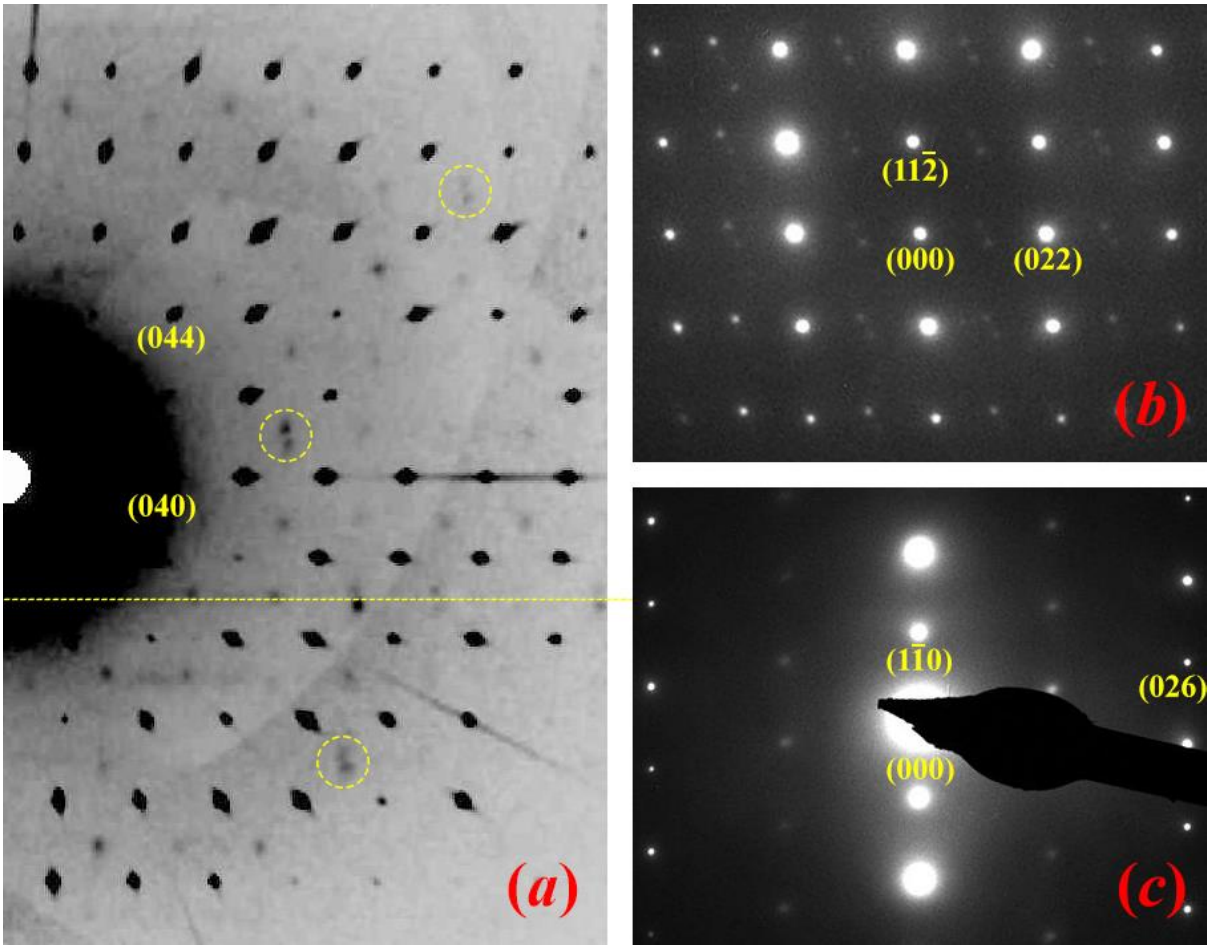

Figure S1 Single-crystal X-ray diffraction pattern and selected area electron diffraction (SAED) patterns of a basalt phenocryst from Mexico (An_{60}) with weak and diffuse *e*-reflections. (*a*) (0*kl*) precession image from X-ray diffraction data. Only a few *e*-reflections pairs (marked with dashed circles) with equal intensities can tell it from an $I\bar{1}$ structure. The XRD data can be reduced and refined as an $I\bar{1}$ structure (wrong model) with a R factor of ~3%; (*b*) [3$\bar{1}$1] zone-axis electron diffraction pattern shows weak but distinct *e*-reflections; (*c*) diffraction pattern of [33$\bar{1}$] zone-axis, in which the *e*-reflections overlaps and looks like *b*-reflections.

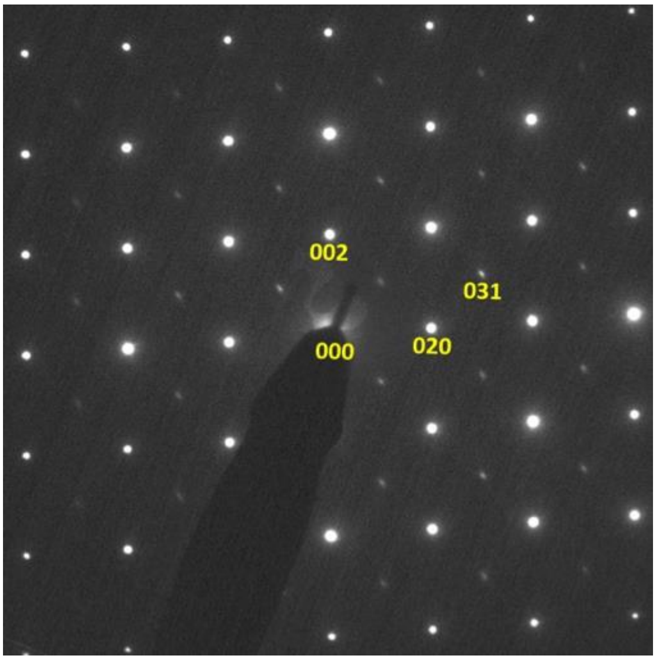

(*a*)

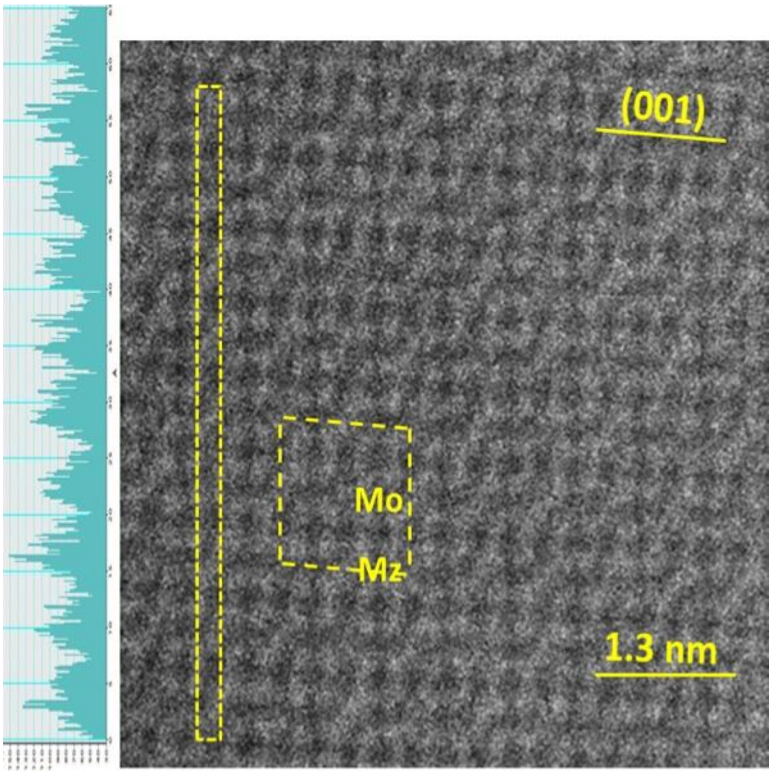

(*b*)

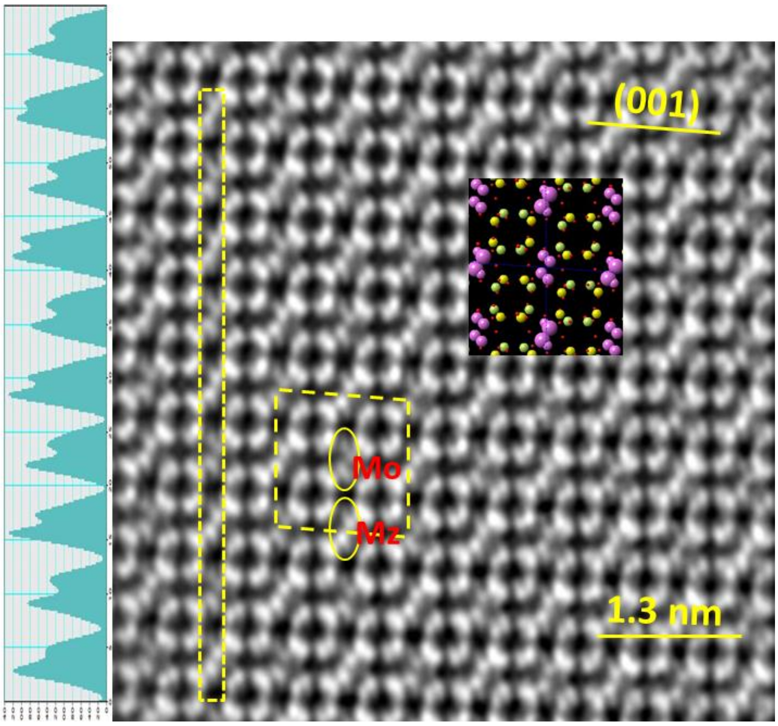

(*c*)

Figure S2 A [100] zone-axis selected-area electron diffraction pattern from the Lake Co. sunstone ($I\bar{1}$) (a), Z-contrast image (b), and its noise-filtered image (c) show Ca-Na ordering in Mzo and Mzi sites based on their intensities (intensity is related to occupancies of Ca and Na and their atomic number, Z^2). Overall intensity from the sum of Mzo and Mzi sites is about 5% stronger than that from the sum of Moo and Moi site (b), which corresponds to about 6% difference in Ca occupancy between the Mo and Mz sites. A structure model is also inserted in the noise-filtered image (c). Big purple spheres are Mzo sites dominated by Ca. The Z-contrast image was obtained by using an aberration-corrected scanning-transmission electron microscope (FEI Titan 80-20).